Naphthalimide-Porphyrin Hybrid Based Ratiometric Bioimaging Probe for Hg2+: Well-Resolved Emission Spectra and Unique Specificity

ARTICLE *in* ANALYTICAL CHEMISTRY · NOVEMBER 2009

Impact Factor: 5.64 · DOI: 10.1021/ac9018445 · Source: PubMed

Anal. Chem. **2009,** *81,* 9993–10001

Naphthalimide−Porphyrin Hybrid Based Ratiometric Bioimaging Probe for Hg^{2+}: Well-Resolved Emission Spectra and Unique Specificity

Chun-Yan Li,[†,‡] Xiao-Bing Zhang,[*,†,§] Li Qiao,[†] Yan Zhao,[†] Chun-Mei He,[†] Shuang-Yan Huan,[†] Li-Min Lu,[†] Li-Xin Jian,[†] Guo-Li Shen,[†] and Ru-Qin Yu[†]

State Key Laboratory of Chemo/Biosensing and Chemometrics, College of Chemistry and Chemical Engineering, Hunan University, Changsha 410082, P. R. China, Key Laboratory of Environmentally Friendly Chemistry and Applications of Ministry of Education, College of Chemistry, Xiangtan University, Xiangtan, 411105, PR China, and State Key Laboratory of Fine Chemicals, Dalian University of Technology, Dalian, 116012, P. R. China

In this paper, we unveil a novel naphthalimide−porphyrin hybrid based fluorescence probe (1) for ratiometric detection of Hg^{2+} in aqueous solution and living cells. The ratiometric signal change of the probe is based on a carefully predesigned molecule containing two independent Hg^{2+}-sensitive fluorophores with their maximal excitation wavelengths located at the same range, which shows reversibly specific ratiometric fluorescence responses induced by Hg^{2+}. In the new developed sensing system, the emissions of the two fluorophores are well-resolved with a 125 nm difference between two emission maxima, which can avoid the emission spectra overlap problem generally met by spectra-shift type probes and is especially favorable for ratiometric imaging intracellular Hg^{2+}. It also benefits from a large range of emission ratios and thereby a high sensitivity for Hg^{2+} detection. Under optimized experimental conditions, the probe exhibits a stable response for Hg^{2+} over a concentration range from 1.0×10^{-7} to 5.0×10^{-5} M, with a detection limit of 2.0×10^{-8} M. The response of the probe toward Hg^{2+} is reversible and fast (response time less than 2 min). Most importantly, the ratiometric fluorescence changes of the probe are remarkably specific for Hg^{2+} in the presence of other abundant cellular metal ions (i.e., Na^+, K^+, Mg^{2+}, and Ca^{2+}), essential transition metal ions in celsl (such as Zn^{2+}, Fe^{3+}, Fe^{2+}, Cu^{2+}, Mn^{2+}, Co^{2+}, and Ni^{2+}), and environmentally relevant heavy metal ions (Ag^+, Pb^{2+}, Cr^{3+}, and Cd^{2+}), which meets the selective requirements for biomedical and environmental monitoring application. The recovery test of Hg^{2+} in real water samples demonstrates the feasibility of the designed sensing system for Hg^{2+} assay in practical samples. It has also been used for ratiometric imaging of Hg^{2+} in living cells with satisfying resolution, which indicates that our novel designed probe has effectively avoided the general emission spectra overlap problem of other ratiometric probes.

Mercury is a major environmental pollutant, as it was estimated by the United Nations Environment Programme (UNEP) that ca. 7500 tons of mercury is released into the environment annually.[1] Mercury ion shows high cellular toxicity due to its strongly biological membrane permeability, and a very small amount of mercury ion could cause serious damage to the central nervous and endocrine systems.[2] Accordingly, the development of methods to detect Hg^{2+} in environmental samples and biological samples such as living cells is of considerable significance and has become the important subject of current chemical research.

Toward both sensing and imaging intracellular Hg^{2+} ion, a fluorescence method might be the best choice by virtue of its high sensitivity, fast analysis with spatial resolution, and non-sample-destructing or less cell damaging.[3−5] Considerable attention has been focused on the design of fluorescent probes for Hg^{2+} ions in the past decade.[3,4] Most of the reported Hg^{2+} probes are based on quenching mechanism owing to the spin−orbit coupling effect.[3] Recently, quite a few Hg^{2+} probes of fluorescence enhancement based on small organic molecule

* To whom correspondence should be addressed. E-mail: xbzhang@hnu.cn. Tel: +86-731-8821903. Fax: +86-731-8821916.

† Hunan University.

‡ Xiangtan University.

§ Dalian University of Technology.

(1) United Nations Environment Programme. *Chemicals: Global Mercury Assessment*; UNEP Chemicals: Geneva, Switzerland, 2002, p 100.

(2) (a) Boening, D. W. *Chemosphere* **2000**, *40*, 1335–1351. (b) Zheng, W.; Aschner, M.; Ghersi-Egea, J.-F. *Toxicol. Appl. Pharmacol.* **2003**, *192*, 1–11. (c) Mutter, J.; Naumann, J.; Schneider, R.; Walach, H.; Haley, B. *Neuroendocrinol. Lett.* **2005**, *26*, 439–446.

(3) (a) Talanova, G. G.; Elkarim, N. S. A.; Talanov, V. S.; Bartsch, R. A. *Anal. Chem.* **1999**, *71*, 3106–3109. (b) Zhang, X. B.; Guo, C. C.; Li, Z. Z.; Shen, G. L.; Yu, R. Q. *Anal. Chem.* **2002**, *74*, 821–825. (c) Moon, S. Y.; Cha, N. R.; Kim, Y. H.; Chang, S.-K. *J. Org. Chem.* **2004**, *69*, 181–183. (d) Moon, S.-Y.; Youn, N. J.; Park, S. M.; Chang, S.-K. *J. Org. Chem.* **2005**, *70*, 2394–2397. (e) Ono, A.; Togashi, H. *Angew. Chem., Int. Ed.* **2004**, *43*, 4300–4302. (f) Zhu, X. J.; Fu, S. T.; Wong, W. K.; Guo, J. P.; Wong, W. Y. *Angew. Chem., Int. Ed.* **2006**, *45*, 3150–3154. (g) He, C. L.; Ren, F. L.; Zhang, X. B.; Han, Z. X. *Talanta* **2006**, *70*, 364–369. (h) Suresh, M.; Ghosh, A.; Das, A. *Chem. Commun.* **2008**, 3906–3908. (i) Niamnont, N.; Siripornnoppakhun, W.; Rashatasakhon, P.; Sukwattanasinitt, M. *Org. Lett.* **2009**, *11*, 2768–2771. (j) Liu, X. J.; Qi, C.; Bing, T.; Cheng, X. H.; Shangguan, D. H. *Anal. Chem.* **2009**, *81*, 3699–3704.

10.1021/ac9018445
Published on Web 11/11/2009

fluorophores,[4] proteins,[6] or oligonucleotides[7] have been developed, as such probes provide off−on responses that are more favorable for bioimaging applications.[4e−g] Unfortunately, most of the fluorescent probes based on single emission intensity changes tend to be affected by a variety of factors, such as instrumental efficiency, probe molecule concentration, its stability under photoillumination, and microenvironment around probe molecule. These limitations can be circumvented by the use of ratiometric probes, which are less prone to suffer such problems. Ratiometric fluorescent probes involve the observation of changes in the ratio of the emission at two wavelengths upon addition of target, which are beneficial for increasing the dynamic range and providing built-in correction for environmental effects. Ratiometric probes for metal ions have been the subjects of a series of investigations in recent years. The analytes reported in the literature include Ca^{2+},[8] Zn^{2+},[9] Ag^{+},[10] Cu^{2+},[11] Cd^{2+},[12] Cr^{3+},[13] and Pb^{2+}.[14] Much effort has also been dedicated to the development of ratiometric probes for Hg^{2+}.[15]

In consideration of the complicated microenvironment in cells, ratiometric fluorescent probes should be more favorable for imaging intracellular metal ions in comparison with fluorescence enhancement probes. However, most reported ratiometric probes were based on emission spectra shift due to internal charge transfer (ICT) or other photochemical process. These spectra-shift type probes in many cases show relatively broad emission spectra with a high degree of overlap before and after binding target ions,[16] which result in poor resolution of the two emission peaks, and, therefore, are not suitable for imaging intracellular metal ions. Only a very few such probes can work well for bioimaging applications.[9c,e,f,12] Ratiometric probes based on a fluorescence resonance energy transfer (FRET) mechanism can theoretically avoid the above-mentioned problems, for which the emission of the donor at relative short wavelength induces emission of the acceptor at longer wavelength with their ratio modulated by the target analytes.[10b,13,15b,e,g,17] A few FRET probes have also been applied in fluorescence bioimaging experiments.[13,16,17b,d] Very recently, the first FRET ratiometric bioimaging probe (chemodosimeter) for Hg^{2+} in living cells was reported by Xiao and Qian by using a BODIPY as donor and a rhodamine as acceptor.[16] However, it showed an irreversible response to Hg^{2+} with a slight interference from Ag^{+} ions. In this paper, we employed a new strategy to solve the spectra overlap problem by linking two independent Hg^{2+}-sensitive fluorophores, pyridine-appended naphthalimide and porphyrin, through covalent bonds. Naphthalimide derivatives are chosen because they are excellent fluorophores with high stability and quantum yield, and some of them show unusually high fluorescence enhancement induced by transition metal ions.[4b,18] A fluoroionophore containing two aminonaphthalimides displayed fluorescence enhancement response toward Hg^{2+} when the excitation wavelength was 410 nm and the emission maximum was 525 nm.[4b] In addition, porphyrins are attractive candidates for metal ion detection owing to their high absorption coefficients and tunable fluo-

(4) (a) Nolan, E. M.; Lippard, S. J. *J. Am. Chem. Soc.* **2003**, *125*, 14270–14271. (b) Guo, X. F.; Qian, X. H.; Jia, L. H. *J. Am. Chem. Soc.* **2004**, *126*, 2272–2273. (c) Yang, Y. K.; Yook, K. J.; Tae, J. *J. Am. Chem. Soc.* **2005**, *127*, 16760–16761. (d) Yoon, S.; Albers, A. E.; Wong, A. P.; Chang, C. J. *J. Am. Chem. Soc.* **2005**, *127*, 16030–16031. (e) Ko, S.-K.; Yang, Y.-K.; Tae, J.; Shin, I. *J. Am. Chem. Soc.* **2006**, *128*, 14150–14155. (f) Yoon, S.; Miller, E. W.; He, Q.; Do, P. H.; Chang, C. J. *Angew. Chem., Int. Ed.,* **2007**, *46*, 6658–6661. (g) Tang, B.; Cui, L. J.; Xu, K. H. *Chembiochem* **2008**, *9*, 1159–1164. (h) Song, F. L.; Watanabe, S.; Floreancig, P. E.; Koide, K. *J. Am. Chem. Soc.* **2008**, *130*, 16460–16461. (i) Nolan, E. M.; Lippard, S. J. *Chem. Rev.* **2008**, *108*, 3443–3480.

(5) (a) Stephens, D. J.; Allan, V. J. *Science* **2003**, *300*, 82–86. (b) Lichtman, J.; Conchello, J. A. *Nat. Methods* **2005**, *2*, 910–919. (c) Giepmans, B. N. G.; Adams, S. R.; Ellisman, M. H.; Tsien, R. Y. *Science* **2006**, *312*, 217–224. (d) Que, E. L.; Domaille, D. W.; Chang, C. J. *Chem. Rev.* **2008**, *108*, 1517–1549. (e) Thoumine, O.; Ewers, H.; Heine, M.; Groc, L.; Frischknecht, R.; Giannone, G.; Poujol, C.; Legros, P.; Lounis, B.; Cognet, L.; Choquet, D. *Chem. Rev.* **2008**, *108*, 1565–1587.

(6) (a) Chen, P.; He, C. *J. Am. Chem. Soc.* **2004**, *126*, 728–729. (b) White, B. R.; Liljestrand, H. M.; Holcombe, J. A. *Analyst* **2008**, *133*, 65–70.

(7) (a) Liu, X.; Tang, Y.; Wang, L.; Zhang, J.; Song, S.; Fan, C.; Wang, S. *Adv. Mater.* **2007**, *19*, 1471–1474. (b) Chiang, C. K.; Huang, C. C.; Liu, C. W.; Chang, H. T. *Anal. Chem.* **2008**, *80*, 3716–3721. (c) Wang, Z. D.; Lee, J. H.; Lu, Y. *Chem. Commun.* **2008**, 6005–6007. (d) Wang, H.; Wang, Y. X.; Jin, J. Y.; Yang, R. H. *Anal. Chem.* **2008**, *80*, 9021–9028. (e) Liu, J. W.; Cao, Z. H.; Lu, Y. *Chem. Rev.* **2009**, *109*, 1948–1998.

(8) (a) Crynkiewicz, G.; Poenie, M.; Tsien, R. Y. *J. Biol. Chem.* **1985**, *260*, 3440–3448. (b) Choi, J. K.; Lee, A.; Kim, S.; Ham, S.; No, K.; Kim, J. S. *Org. Lett.* **2006**, *8*, 1601–1604.

(9) (a) Yang, R. H.; Li, K. A.; Wang, K. M.; Zhao, F. L.; Li, N.; Liu, F. *Anal. Chem.* **2003**, *75*, 612–621. (b) Ajayaghosh, A.; Carol, P.; Sreejith, S. *J. Am. Chem. Soc.* **2005**, *127*, 14962–14963. (c) Komatsu, K.; Urano, Y.; Kojima, H.; Nagano, T. *J. Am. Chem. Soc.* **2007**, *129*, 13447–13454. (d) Li, C. Y.; Zhang, X. B.; Dong, Y. Y.; Ma, Q. J.; Shen, G. L.; Yu, R. Q. *Anal. Chim. Acta* **2008**, *616*, 214–221. (e) Roussakis, E.; Voutsadaki, S.; Pinakoulaki, E.; Sideris, D. P.; Tokatlidis, K.; Katerinopoulos, H. E. *Cell Calcium* **2008**, *44*, 270–275. (f) Nolan, E. M.; Lippard, S. J. *Acc. Chem. Res.* **2009**, *42*, 193–203. (g) Xue, L.; Liu, C.; Jiang, H. *Chem. Commun.* **2009**, 1061–1063.

(10) (a) Yang, R. H.; Chan, W. H.; Lee, A. W. M.; Xia, P. F.; Zhang, H. K.; Li, K. A. *J. Am. Chem. Soc.* **2003**, *125*, 2884–2885. (b) Coskun, A.; Akkaya, E. U. *J. Am. Chem. Soc.* **2005**, *127*, 10464–10465. (c) Liu, L.; Zhang, D. Q.; Zhang, G. X.; Xiang, J. F.; Zhu, D. B. *Org. Lett.* **2008**, *10*, 2271–2274.

(11) (a) Royzen, M.; Dai, Z.; Canary, J. W. *J. Am. Chem. Soc.* **2005**, *127*, 1612–1613. (b) Xu, Z. C.; Xiao, Y.; Qian, X. H.; Cui, J. N.; Cui, D. W. *Org. Lett.* **2005**, *7*, 889–892. (c) Xu, Z. C.; Qian, X. H.; Cui, J. N. *Org. Lett.* **2005**, *7*, 3029–3032. (d) Shao, N.; Jin, J. Y.; Wang, H.; Zhang, Y.; Yang, R. H.; Chan, W. H. *Anal. Chem.* **2008**, *80*, 3466–3475. (e) Lin, W. Y.; Yuan, L.; Tan, W.; Feng, J. B.; Long, L. L. *Chem.—Eur. J.* **2009**, *15*, 1030–1035.

(12) (a) Peng, X. J.; Du, J. J.; Fan, J. L.; Wang, J. Y.; Wu, Y. K.; Zhao, J. Z.; Sun, S. G.; Xu, T. *J. Am. Chem. Soc.* **2007**, *129*, 1500–1501. (b) Taki, M.; Desaki, M.; Ojida, A.; Iyoshi, S.; Hirayama, T.; Hamachi, I.; Yamamoto, Y. *J. Am. Chem. Soc.* **2008**, *130*, 12564–12565.

(13) Zhou, Z. G.; Yu, M. X.; Yang, H.; Huang, K. W.; Li, F. Y.; Yi, T.; Huang, C. H. *Chem. Commun.* **2008**, 3387–3389.

(14) (a) Deo, S.; Godwin, H. A. *J. Am. Chem. Soc.* **2000**, *122*, 174–175. (b) Roussakis, E.; Pergantis, S. A.; Katerinopoulos, H. E. *Chem. Commun.* **2008**, 6221–6223.

(15) (a) Nolan, E. M.; Lippard, S. J. *J. Mater. Chem.* **2005**, *15*, 2778–2783. (b) Coskun, A.; Akkaya, E. U. *J. Am. Chem. Soc.* **2006**, *128*, 14474–14475. (c) Nolan, E. M.; Lippard, S. J. *J. Am. Chem. Soc.* **2007**, *129*, 5910–5918. (d) Wegner, S. V.; Okesli, A.; Chen, P.; He, C. *J. Am. Chem. Soc.* **2007**, *129*, 3474–3475. (e) Shang, G. Q.; Gao, X.; Chen, M. X.; Zheng, H.; Xu, J. G. *J. Fluoresc.* **2008**, *18*, 1187–1192. (f) Tian, M.; Ihmels, H. *Chem. Commun.* **2009**, 3175–3177. (g) Guliyev, R.; Coskun, A.; Akkaya, E. U. *J. Am. Chem. Soc.* **2009**, *131*, 9007–9013. (h) Coskun, A.; Yilmaz, M. D.; Akkaya, E. U. *Org. Lett.* **2007**, *9*, 607–609. (i) Han, Z. X.; Luo, H. Y.; Zhang, X. B.; Kong, R. M.; Shen, G. L.; Yu, R. Q. *Spectrochim. Acta Part A* **2009**, *72*, 1084–1088.

(16) Zhang, X. L.; Xiao, Y.; Qian, X. H. *Angew. Chem., Int. Ed.* **2008**, *47*, 8025–8029.

(17) (a) Kawanishi, Y.; Kikuchi, K.; Takakusa, H.; Mizukami, S; Urano, Y.; Higuchi, T. *Nagano T Angew. Chem., Int. Ed.* **2000**, *39*, 3438–3440. (b) Kikuchi, K.; Takakusa, H.; Nagano, T. *Trends Anal. Chem.* **2004**, *23*, 407–415. (c) Albers, A. E.; Okreglak, V. S.; Chang, C. J. *J. Am. Chem. Soc.* **2006**, *131*, 9640–9641. (d) Han, J. Y.; Loudet, A.; Barhoumi, R.; Burghardt, R. C.; Burgess, K. *J. Am. Chem. Soc.* **2009**, *131*, 1642–1643.

(18) (a) Ramachandram, B.; Saroja, G.; Sankaran, N. B.; Samanta, A. *J. Phys. Chem. B* **2000**, *104*, 11824–11832. (b) Abad, S.; Kluciar, M.; Miranda, M. A.; Pischel, U. *J. Org. Chem.* **2005**, *70*, 10565–10568. (c) Zhu, W. P.; Xu, Y. F.; Qian, X. H. *Prog. Chem.* **2007**, *19*, 1229–1238.

Scheme 1. Chemical Structure and Synthetic Route of Compounds 1 and 2

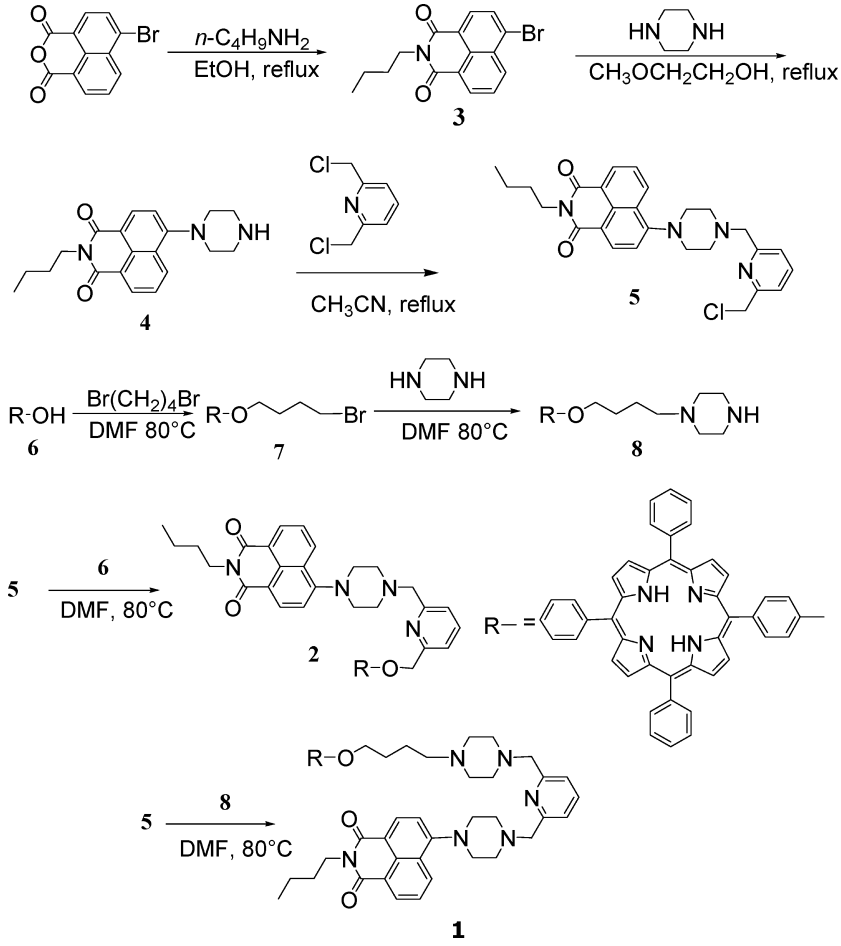

rescence emission.[19] We have reported that a molecule possessing two porphyrins in a PVC matrix shows a fluorescence quenching response toward Hg^{2+} at 650 nm when the excitation wavelength was 420 nm.[3b] Herein we report the synthesis and application of our novel designed naphthalimide−porphyrin hybrid based Hg^{2+} probe **1** (Scheme 1). It shows a reversible ratiometric fluorescence response for Hg^{2+} in neutral aqueous environment with remarkably high selectivity. Moreover, this hybrid probe achieved well-resolved emission spectra with a 125 nm difference between two emission peaks, which benefits from observation of fluorescence signal change at two different wavelengths with high resolution. As a proof-of-concept, the proposed probe has been further applied for ratiometric imaging of Hg^{2+} in living cells with satisfying resolution.

EXPERIMENTAL SECTION

Reagents and Apparatus. *N*,*N*-Dimethylformamide (DMF) was distilled from CaH_2 under reduced pressure and stored over 4 Å molecular sieves, and acetonitrile was distilled over phosphorus oxide prior to use. All chemicals were purchased from commercial suppliers and used without further purification. Twice-distilled water was used throughout all experiments. Column chromatography was conducted over silica gel (200−300 mesh), and thin layer chromatography (TLC) was carried out using silica gel 60 F254, both of which were obtained from the Qingdao Ocean Chemicals (Qingdao, China). ^1H, ^{13}C NMR spectra were recorded on a Bruker DRX-400 spectrometer operating at 400 and 100 MHz, respectively, with tetramethylsilane as an internal reference. All chemical shifts are reported in the standard δ notation of parts per million. LC−MS analyses were performed using an Agilent 1100 HPLC/MSD spectrometer; UV−vis absorption spectra were recorded with a Shimadzu MultiSpec-1501 spectrophotometer. All fluorescence measurements were conducted on a Hitachi F-4500 fluorescence spectrometer with excitation slit set at 10.0 nm and emission at 5.0 nm. Fluorescence images of Hela cells were carried out with an Olympus FV500 confocal microscope. The pH measurements were carried out on a Mettler-Toledo Delta 320 pH meter.

Spectrophotometric Experiments and Association Constants. Due to the weak water solubility of porphyrin derivatives, both the fluorescence and UV−vis absorption spectra experiments were conduct in a water/ethanol (1:1, v/v) solution. The fluorescence emission spectra were recorded at an excitation wavelength of 415.0 nm with an emission wavelength range from 450.0 to 700.0 nm. A 2×10^{-5} M stock solution of **1** was prepared by dissolving **1** in absolute ethanol. A stock standard solution of Hg^{2+} (0.01 M) was prepared by dissolving an appropriate amount of mercury nitrate in water and adjusting the volume to 500 mL in a volumetric flask. This was further diluted to 1×10^{-3}−1×10^{-7} M stepwise. The complex solution of Hg^{2+}/**1** was prepared

(19) (a) Grigg, R.; Norbert, W. D. J. A. *Chem. Commun.* **1992**, 1298–1300. (b) Beletskaya, I.; Tyurin, V. S.; Tsivadze, A. Y.; Guilard, R.; Stern, C. *Chem. Rev.* **2009**, *109*, 1659–1713.

by adding 5.0 mL of the stock solution of **1** and 1.0 mL of the stock solution of Hg^{2+} in a 10 mL volumetric flask. Then the mixture was diluted to 10 mL with Tris-HNO_3 buffer solution. In the solution thus obtained, the concentrations were 1×10^{-5} M in **1** and $(1 \times 10^{-3}) - (1 \times 10^{-8})$ M in Hg^{2+}. The solution was protected from light and kept at 4 °C for further use. A blank solution of **1** was prepared under the same conditions without Hg^{2+}.

The obtained data of the fluorescence emission intensity of **1** at 650 and 525 nm were separately analyzed for apparent association constants K_1 for porphyrin and K_2 for naphthalimide moiety, respectively,[3b] using the relationships that are established with the formation of a *m*:*n* metal-to-ligand complex.

$$\frac{\alpha^n}{1-\alpha} = \frac{1}{nK[\mathrm{L}]_t^{n-1}[\mathrm{M}]^m} \quad (1)$$

Here [M] and [L] denote the free concentration of the Hg^{2+} ion and the ligand (porphyrin or naphthalimide moiety in compound **1**), respectively. The relative fluorescence intensity α is defined as the ratio of free ligand, $[L]_f$, to the total amount of ligand, $[L]_t$ in the solution. It can be experimentally determined by measuring the fluorescence intensity of **1** at 650 and 525 nm in the presence of different concentrations of Hg^{2+}, respectively

$$\alpha = \frac{[\mathrm{L}]_f}{[\mathrm{L}]_t} = \frac{F - F_0}{F_b - F_0} \quad (2)$$

where F_b and F_0 are limiting values of the fluorescence intensity at 650 nm for the porphyrin moiety or at 525 nm for naphthalimide unit at zero metal ion concentration and at final (plateau) metal ion concentration, respectively. F is the corresponding fluorescence intensity at 650 or 525 nm of the probe actually measured when contacting with a metal ion solution of a given concentration.

Preparation of Cell Cultures and Fluorescence Imaging Experiments. The living Hela cells were obtained from the biomedical engineering center of Hunan University (Changsha, China). Immediately prior to the imaging experiments, the cells were washed with phosphate-buffered saline (PBS), incubated with 10 μM compound **1** (in the culture medium containing 2% DMSO) for 1 h at 37 °C and then washed with phosphate-buffered saline (PBS) three times and imaged. After being incubating with 10 μM $Hg(NO_3)_2$ for another 1 h at 37 °C, the Hela cells were rinsed with PBS three times and imaged again. Confocal fluorescence imaging of intracellular Hg^{2+} in Hela cells was observed under an OLYMPUS FV500 confocal microscope. The excitation wavelength of laser was 450 nm. Emissions were centered at 515 ± 10 and 650 ± 10 nm (double channel).

Synthesis of Compound 3. 4-Bromo-1,8-naphthalic anhydride (2.76 g, 10 mmol) and *n*-butylamine (0.73 g, 10 mmol) were dissolved in ethanol (20 mL). The reaction mixture was stirred and refluxed for 2 h. After the solvent was evaporated under reduced pressure, the crude product was purified by silica gel column chromatography using CH_2Cl_2/petroleum ether (1:1, v/v) as eluent to afford a solid product: yield 2.83 g (85%); ^{1}H NMR (400 MHz, $CDCl_3$) δ 8.64 (dd, J = 7.2 Hz, 1H), 8.55 (dd, J = 8.4 Hz, 1H), 8.40 (d, J = 8.0 Hz, 1H), 8.03 (d, J = 7.6 Hz, 1H), 7.82−7.86 (m, 1H), 4.17 (t, J = 7.6 Hz, 2H), 1.68−1.75 (m, 2H), 1.40−1.50 (m, 2H), 0.98 (t, J = 8.0 Hz, 3H); MS (EI) *m*/*z* 331.

Synthesis of Compound 4. Piperazine (1.29 g, 15 mmol) was dissolved in methylglycol (30 mL), and compound **3** (0.99 g, 3.0 mmol) was added. The reaction mixture was stirred and refluxed for 4 h under nitrogen atmosphere. After the solvent was evaporated under reduced pressure, the crude product was purified by silica gel column chromatography using CH_2Cl_2/EtOH (10:1, v/v) as eluent to afford a yellow solid: yield 0.76 g (75%); ^{1}H NMR (400 MHz, $CDCl_3$) δ 8.59 (dd, J = 7.2 Hz, 1H), 8.52 (d, J = 8.0 Hz, 1H), 8.42 (dd, J = 7.6 Hz, 1H), 7.70 (q, J = 8.4 Hz, 1H), 7.22 (d, J = 8.0 Hz, 1H), 4.17 (t, J = 7.6 Hz, 2H), 3.70−3.75 (m, 4H), 3.20−3.24 (m, 2H), 1.67−1.75 (m, 2H), 1.40−1.49 (m, 2H), 0.97 (t, J = 7.2 Hz, 3H); MS (EI) *m*/*z* 337.

Synthesis of Compound 5. 2,6-Bis(chloromethyl)pyridine (525 mg, 3.0 mmol) was dissolved in acetonitrile (20 mL), and compound **4** (337 mg, 1.0 mmol) was added. The reaction mixture was stirred and refluxed for 6 h. After the solvent was evaporated under reduced pressure, the crude product was purified by silica gel column chromatography using CH_2Cl_2/EtOH (100:1, v/v) as eluent to afford a yellow solid: yield 300 mg (63%); ^{1}H NMR (400 MHz, $CDCl_3$) δ 8.57 (dd, J = 7.6 Hz, 1H), 8.51 (d, J = 8.0 Hz, 1H), 8.40 (d, J = 8.4 Hz, 1H), 7.75 (t, J = 7.6 Hz, 1H), 7.68 (t, J = 8.0 Hz, 1H), 7.47 (d, J = 7.6 Hz, 1H), 7.41 (d, J = 7.6 Hz, 1H), 7.21 (d, J = 8.0 Hz, 1H), 4.70 (s, 2H), 4.16 (t, J = 7.6 Hz, 2H), 3.84 (s, 2H), 3.34 (s, 4H), 2.88 (s, 4H), 1.67−1.74 (m, 2H), 1.40−1.49 (m, 2H), 0.97 (t, J = 7.2 Hz, 3H); ^{13}C NMR (100 MHz, $CDCl_3$) δ 164.4, 164.0, 156.2, 155.8, 137.5, 132.4, 131.0, 130.2, 129.8, 126.1, 125.6, 123.3, 122.5, 121.3, 114.9, 64.2, 53.3, 53.0, 46.8, 40.1, 30.2, 20.3, 13.8; HRMS *m*/*z* calcd for $C_{27}H_{29}ClN_4O_2$ (M + H) 477.1979, found 477.1984.

Synthesis of Compound 6. Compound **6** was synthesized according to a reported procedure.[20]

Synthesis of Compound 7. 1,4-Dibromobutane (432 mg, 2.0 mmol) and potassium carbonate (276 mg, 2.0 mmol) were dissolved in *N*,*N*-dimethylformamide (10 mL), and compound **6** (252 mg, 0.4 mmol) was added. The reaction mixture was stirred for 3 h at 80 °C. After the solvent was evaporated under reduced pressure, the crude product was purified by silica gel column chromatography using CH_2Cl_2 as eluent to afford a purple solid: yield 257 mg (84%); ^{1}H NMR (400 MHz, $CDCl_3$) δ 8.88 (s, 2H), 8.84 (s, 6H), 8.22 (d, J = 7.6 Hz, 6H), 8.12 (d, J = 8.8 Hz, 2H), 7.73−7.78 (m, 9H), 7.27 (d, J = 8.0 Hz, 2H), 4.29 (t, J = 6.0 Hz, 2H), 3.63 (t, J = 6.0 Hz, 2H), 2.22−2.28 (m, 2H), 2.13−2.18 (m, 2H), −2.78 (s, 2H).

Synthesis of Compound 8. Piperazine (86 mg, 1.0 mmol) was dissolved in *N*,*N*-dimethylformamide (10 mL), and compound **7** (153 mg, 0.2 mmol) was added. The reaction mixture was stirred for 6 h at 80 °C under nitrogen atmosphere. After the solvent was evaporated under reduced pressure, the crude product was purified by silica gel column chromatography using CH_2Cl_2/EtOH (20:1, v/v) as eluent to afford a purple solid: yield 174 mg (72%); ^{1}H NMR (400 MHz, $CDCl_3$) δ 8.87 (s, 2H), 8.84 (s, 6H), 8.21 (d, J = 7.6 Hz, 6H), 8.10 (d, J = 8.0 Hz, 2H), 7.71−7.77 (m,

(20) Adler, A. D.; Longo, F. R.; Finarelli, J. D.; Goldmacher, J.; Assour, J.; Korsakoff, L. *J. Org. Chem.* **1967**, *32*, 476.

9H), 7.22 (d, J = 8.4 Hz, 2H), 4.21 (s, 2H), 3.32 (s, 4H), 2.90 (s, 4H), 2.65 (s, 2H), 1.96 (s, 2H), 1.85 (s, 2H), −2.77 (s, 2H); ^{13}C NMR (100 MHz, $CDCl_3$) δ 161.0, 142.2, 135.6, 134.6, 131.0, 127.7, 126.7, 120.1, 112.7, 67.7, 51.8, 50.6, 45.0, 29.7, 27.5; HRMS m/z calcd for $C_{52}H_{46}N_6O$ (M + H) 771.3733, found 771.3721.

Synthesis of Compound 2. Compound **5** (95 mg, 0.2 mmol) and compound **6** (126 mg, 0.2 mmol) were dissolved in *N*,*N*-dimethylformamide (10 mL). The reaction mixture was stirred for 6 h at 80 °C. After the solvent was evaporated under reduced pressure, the crude product was purified by silica gel column chromatography using CH_2Cl_2/EtOH (50:1, v/v) as eluent to afford a purple solid: yield 173 mg (81%); ^{1}H NMR (400 MHz, $CDCl_3$) δ 8.85 (s, 2H), 8.84 (s, 6H), 8.59 (d, J = 7.2 Hz, 1H), 8.53 (d, J = 8.0 Hz, 1H), 8.47 (d, J = 8.0 Hz, 1H), 8.20−8.23 (m, 6H), 8.15 (d, J = 8.4 Hz, 2H), 7.99 (d, J = 7.2 Hz, 1H), 7.73−7.80 (m, 10H), 7.40 (d, J = 8.8 Hz, 2H), 7.26 (d, J = 8.0 Hz, 2H), 7.22 (d, J = 7.2 Hz, 1H), 5.53 (s, 2H), 4.15 (s, 2H), 3.93 (s, 2H), 3.37 (s, 4H), 2.93 (s, 4H), 1.67−1.73 (m, 2H), 1.40−1.47 (m, 2H), 0.96 (t, J = 7.2 Hz, 3H), −2.80 (s, 2H); ^{13}C NMR (100 MHz, $CDCl_3$) δ 164.0, 158.3, 157.0, 142.2, 137.5, 135.7, 135.1, 134.6, 132.5, 131.0, 130.1, 129.8, 127.7, 126.7, 126.1, 125.6, 123.2, 120.1, 119.8, 114.9, 113.1, 60.5, 53.4, 53.0, 40.1, 30.2, 29.7, 20.4, 13.9; HRMS m/z calcd for $C_{75}H_{66}N_{10}O_3$ (M + H) 1155.5319, found 1155.5311.

Synthesis of Compound 1. Compound **5** (95 mg, 0.2 mmol) and compound **8** (155 mg, 0.2 mmol) were dissolved in *N*,*N*-dimethylformamide (DMF) (10 mL). The reaction mixture was stirred for 6 h at 80 °C. After the solvent was evaporated under reduced pressure, the crude product was purified by silica gel column chromatography using CH_2Cl_2/EtOH (20:1, v/v) as eluent to afford a purple solid: yield 189 mg (78%); ^{1}H NMR (400 MHz, $CDCl_3$) δ 8.88 (s, 2H), 8.84 (s, 6H), 8.56 (d, J = 7.6 Hz, 1H), 8.50 (d, J = 8.0 Hz, 1H), 8.39 (d, J = 8.0 Hz, 1H), 8.22 (d, J = 7.2 Hz, 6H), 8.11 (d, J = 8.4 Hz, 2H), 7.72−7.78 (m, 10H), 7.65−7.68 (m, 2H), 7.35 (d, J = 8.0 Hz, 2H), 7.26 (d, J = 8.4 Hz, 2H), 7.20 (d, J = 8.4 Hz, 1H), 4.27 (t, J = 6.0 Hz, 2H), 4.15 (t, J = 7.6 Hz, 2H), 3.81 (s, 2H), 3.74 (s, 2H), 3.31 (s, 4H), 2.84 (s, 4H), 2.64 (s, 4H), 2.56 (d, J = 7.2 Hz, 4H), 2.29−2.34 (m, 2H), 1.97−2.03 (m, 4H), 1.67−1.74 (m, 2H), 1.39−1.47 (m, 2H), 0.96 (t, J = 7.2 Hz, 3H), −2.78 (s, 2H); ^{13}C NMR (100 MHz, $CDCl_3$) δ 164.4, 164.0, 160.7, 157.4, 155.8, 137.0, 134.5, 132.4, 131.0, 130.1, 129.8, 126.6, 126.1, 125.6, 123.2, 121.7, 121.6, 116.8, 114.9, 68.6, 64.3, 64.2, 53.6, 53.3, 52.9, 52.4, 45.5, 40.0, 39.9, 30.2, 29.6, 20.3, 13.8; HRMS m/z calcd for $C_{79}H_{74}N_{10}O_3$ (M + H) 1211.5945, found 1211.5958.

RESULTS AND DISCUSSION

Synthesis and Characteristics of Probe Molecules. The synthetic routes for fluorescent probe **1** and analogue compound **2** are depicted in Scheme 1. Compound **3**,[11b] **4**,[4b] **6**,[20] and **7**[3b] were synthesized following literature procedures with some modifications. As an intermediate for both compound **1** and **2**, compound **5** was first synthesized through three steps with 4-bromo-1,8-naphthalic anhydride as a starting material in a satisfying overall yield. It was then either directly coupled with a single hydroxyl-functionalized *meso*-tetraphenylporphyrin **6** through a nucleophilic substitution reaction to give compound **2** in 73% yield or reacted with a new synthesized single piperazinylbutyloxyl-functionalized *meso*-tetraphenylporphyrin **8** to afford compound **1** in 78% yield. Compound **8** was prepared from compound **6**, piperazine, and 1,4-dibromobutane through two steps of asymmetrical nucleophilic substitution reactions under mild conditions with good selectivity and satisfying yield. The structures of all synthesized compounds were identified by MS data, ^{1}H NMR and ^{13}C NMR spectrum (see Supporting Information).

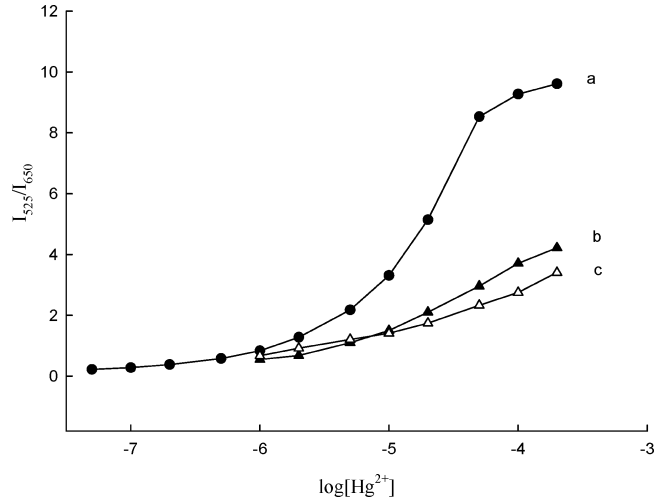

Figure 1. Changes in the fluorescence intensity of compound **1** (a), **2** (b), and the mixture of **5** and **8** (c) at 525 nm versus that at 650 nm upon addition of different concentrations of Hg^{2+}, respectively.

Mercury Ion-Induced Ratiometric Fluorescence Response of 1 and 2. The design of synthetic fluorescent probes for ratiometric measurement of mercury ion has been a challenging task. ICT and FRET mechanisms have been widely utilized to develop ratiometric fluorescent probes for various targets. To obtain well-resolved emission peaks of fluorophore and to avoid the emission spectra overlap problem generally met by ICT probes, we employed a new strategy to prepare a Hg^{2+}-sensitive ratiometric fluorescent probe by connecting two independent Hg^{2+}-sensitive fluorophores, naphthalimide and porphyrin (their excitation maxima located at the same range), through covalent bonds. For optimization purposes, two probe molecules (compound **1** and **2**) with different linkers were designed and synthesized (Scheme 1). The small distance between two fluorophores in compound **2** results in larger steric hindrance, which caused difficulty for compound **2** to bind Hg^{2+} and resulted in a small fluorescence intensity ratio change at 525 nm (indicating naphthalimide emission) versus that at 650 nm (indicating porphyrin emission, Figure 1, curve b). In contrast, the longer distance between two fluorophores in compound **1** seems to be beneficial for obtaining remarkable ratiometric change of fluorescence intensities when Hg^{2+} is introduced (Figure 1, curve a). To further investigate the difference binding capability with Hg^{2+} between compound **1** and **2**, their UV−vis absorption spectra before and after addition of excess Hg^{2+} were recorded (see Supporting Information, Figure S1). Compared to compound **2**, compound **1** shows a more significant and substantial change of absorption spectral features upon the interaction with Hg^{2+}. This indicated that compound **1** could bind with Hg^{2+} more strongly than compound **2**, which is the rational explanation for the variation of fluorescence intensity changes of the above-mentioned compounds induced by Hg^{2+}. On the basis of the aforementioned reasoning, concerning the

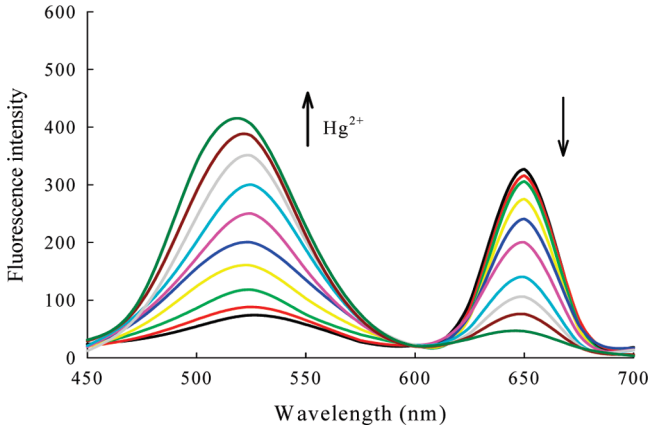

Figure 2. The fluorescence emission spectra of **1** (10 μM) in the presence of different concentrations of Hg^{2+} (0, 0.1, 0.2, 0.5, 1, 2, 5, 10, 20, 50 μM) in buffered (Tris-HNO_3, pH 7.0) water/ethanol (1:1, v/v) solution. The excitation wavelength was fixed at 415.0 nm.

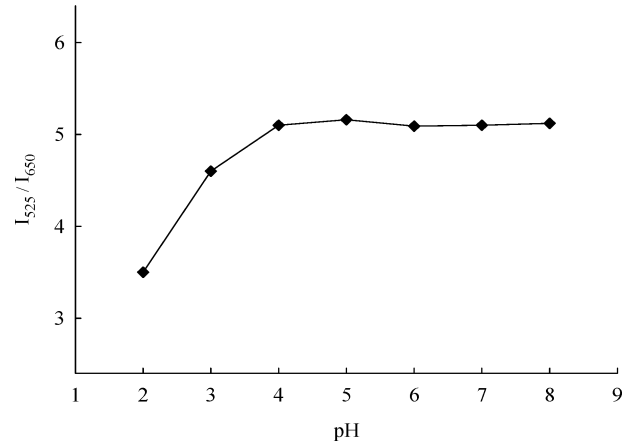

Figure 3. Effect of pH on the fluorescence intensity at 525 nm to that at 650 nm of **1** (10 μM) in the presence of Hg^{2+} (20 μM).

variation of ratiometric fluorescence intensity change of the compounds involved, compound **1** was chosen for further studies.

We further compared the sensing performance of the hybrid molecule with the individual naphthalimide (compound **5**) and porphyrin molecules (compound **8**). As shown in Figure 1 (curve c), fluorescence intensity ratio change of the mixture solution of compound **5** and coupound **8** (from 0.67 to 3.41) was much lower than that of the coupound **1** (from 0.83 to 9.61) with the concentration of Hg^{2+} changed from 1 to 200 μM. This low ratio change might be due to the poor water solubility of the porphyrin derivative. Small fluorescence change was observed when Hg^{2+} was added to coupound **8** in the buffered (Tris-HNO_3, pH = 7.0) water/ethanol (1:1, v/v) solution (see Supporting Information, Figure S2); therefore, our original report using porphyrin dimer for Hg^{2+} sensing was only performed well in a PVC matrix.[3b] Interestingly, by linking the two compounds together, the water solubility of the hybrid improved significantly; after addition of the Hg^{2+}, the remarkable decrease of emission at 650 nm and significant increase of the emission at 525 nm happened simultaneously, resulting in a huge ratio increase from 0.28 to 9.61, with the concentration of Hg^{2+} changed from 0.1 to 200 μM (Figure 1, curve c).Therefore, the hybrid molecule is not a simple combination of the two molecules, but has improved solubility and much enhanced sensing performance. Most importantly, this new hybrid is more favorable for the fluorescence ratiometric imaging of Hg^{2+}, especially in living cells, where two individual fluorophores might have different permeability toward cellular membranes, and therefore, the local concentrations of the two individual fluophores might vary a lot in the cellular environment.

Figure 2 shows the fluorescence spectra of **1** exposed to buffered (Tris-HNO_3, pH = 7.0) water/ethanol (1: 1, v/v) solutions containing different concentrations of Hg^{2+} recorded at excitation wavelength of 415.0 nm and emission wavelength of 450.0−700.0 nm. The spectrum of **1** without Hg^{2+} exhibits two typical fluorescence emission peaks at 525 and 650 nm, which are due to the naphthalimide and porphyrin moieties, respectively. As shown in Figure 2, the two emission peaks are well-resolved with a 125 nm difference, indicating that our new strategy for the ratiometric Hg^{2+} probe has effectively avoided the emission spectra overlap problem usually met by spectra-shift-type probes, which is especially favorable for ratiometric imaging of intracellular Hg^{2+} and also benefits from a large range of emission ratios and thereby a high sensitivity for Hg^{2+} detection. Experimental results show that the addition of Hg^{2+} to a solution of **1** indeed induces a remarkable increase of fluorescence signal at 525 nm and the decrease of that at 650 nm. The emission intensity ratio, I_{525}/I_{650}, was gradually increased with increasing Hg^{2+} concentration (Figure 1). The dynamic response concentration range for Hg^{2+} covers from 1.0 $\times 10^{-7}$ to 5.0 $\times 10^{-5}$ M, with a detection limit of 2.0 $\times 10^{-8}$ M (3σ/slope).

The Effect of Acidity on the Performance of Probe. The pH value of the environment around the fluorescent probe usually shows somewhat of an effect on its performance toward target metal ion due to the protonation or deprotonation reaction for the fluorophore and the hydrolysis reaction for the metal ions in the basic condition. The effects of pH on the fluorescence response of the new probe **1** to Hg^{2+} were therefore investigated. A solution of the high concentration of Hg^{2+} might cause precipitation of HgO in the alkaline condition, so these experiments were carried out at a pH range from 2.0 to 8.0, with the concentration of **1** fixed at 10 μM and of Hg^{2+} at 20 μM, respectively (Figure 3). In the section of lower pH value from 2.0 to 4.0, the fluorescence intensity ratio of **1** decreased with decreasing pH value, which might be caused by the protonation of compound **1**, and thus, its binding capability was lower with the metal ions. In a wide range of pH from 4.0 to 8.0, acidity does not affect the determination of Hg^{2+} with compound **1**. In other words, there is no need for strict control of the pH value of sample solution for determining of Hg^{2+}, which is convenient for practical applications of the proposed probe in determination of Hg^{2+} in actual samples.

Selectivity. Achieving highly selective response to the analyte of interest over other potentially competing species coexisting in the sample is a necessity for a bioimaging probe with potential application in biomedical and environmental systems. Therefore, the selectivity and competition experiments were extended to various metal ions, such as abundant cellular cations (Na^+, K^+, Mg^{2+}, and Ca^{2+}), essential transition metal ions in cells (Zn^{2+}, Fe^{3+}, Fe^{2+}, Cu^{2+}, Mn^{2+}, Co^{2+}, and Ni^{2+}), and environmentally relevant heavy metal ions (Ag^+, Pb^{2+}, Cr^{3+}, and Cd^{2+}). The

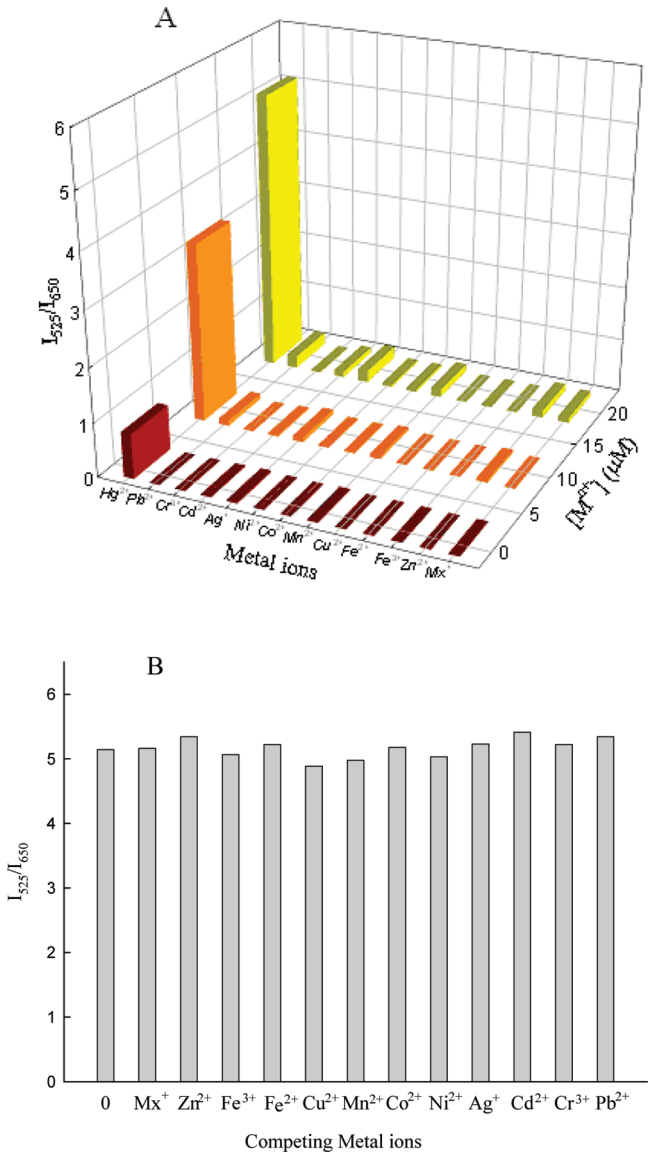

Figure 4. The selectivity of **1** (10 μM) to Hg^{2+} over competing metal ions. (a) The changes of fluorescence intensity ratio of **1** upon the addition of three concentrations (1, 10, and 20 μM) of different metal ions. (b) The fluorescence intensity ratio of **1** (10 μM) with Hg^{2+} (20 μM) in the presence of competing metal ions (10 mM for Na^+, K^+, Mg^{2+}, Ca^{2+} and 200 μM for others). Mx is a mixture of K^+, Na^+, Mg^{2+}, and Ca^{2+}.

selectivity was first tested with excitation fixed at 415 nm, and the fluorescent response (I_{525}/I_{650}) was recorded to the above-mentioned 15 competing metal ions at concentrations of 1, 10, and 20 μM, respectively. As shown in Figure 4A, with all three concentrations being considered, little fluorescence intensity ratio change was observed with all above-mentioned biomedically relevant or environmentally relevant metal ions, indicating that our proposed probe exhibits high selectivity to Hg^{2+} over other competing metal ions. In certain environmental samples, such as river water and seawater, the concentrations of some other contaminating metal ions, such as Fe^{3+}, Cu^{2+}, and Zn^{2+}, are significantly higher than that of Hg^{2+}, so selective detection of Hg^{2+} in the presence of these metal ions with high concentration is a challenge for most common probes. To test the practical applicability of our fluorescent probe for Hg^{2+},

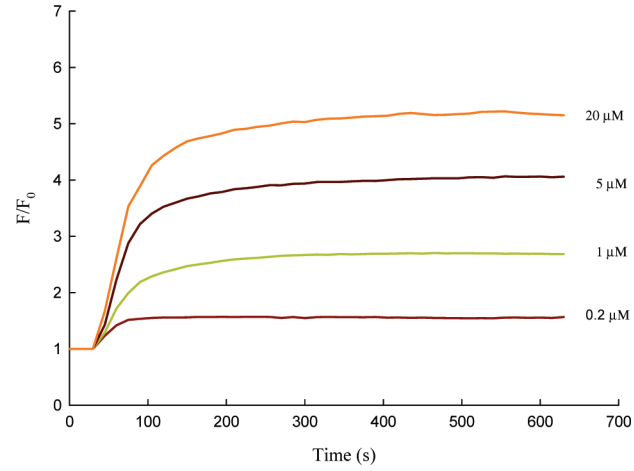

Figure 5. Kinetics of the fluorescence enhancement of **1** (10 μM) in the presence of different concentrations of Hg^{2+}. Fluorescence intensity was recorded at 525.0 nm. Excitation wavelength was fixed at 415.0 nm.

competition experiments were also carried out. An excess amount of above-mentioned metal ions (10 mM for Na^+, K^+, Mg^{2+}, Ca^{2+} and 200 μM for others) are added to 20 μM Hg^{2+} in buffered water/ethanol solution and the fluorescence response (I_{525}/I_{650}) of the probe was detected and then compared with that of buffer solution containing only 20 μM Hg^{2+}. Results are shown in Figure 4B. Our probe showed almost unchanged responses to Hg^{2+} before and after addition of other competing metal ions. These experimental results show that the response of the probe to Hg^{2+} is unaffected by the presence of the other possible contaminating metal ions, even those existing in a concentration 10 times higher than that of Hg^{2+}. All these results indicate that our proposed probe is highly selective and has great potential for biomedical and environmental applications.

Response Time and Hg^{2+} Binding Reversibility for 1. Besides high sensitivity and selectivity, a short response time and reversible response are other two necessities for a fluorescent probe to dynamically image intracellular Hg^{2+} ions or monitor Hg^{2+} in environmental samples in real time. To study the response time of the naphthalimide−porphyrin hybrid based fluorescence probe **1** to Hg^{2+}, the kinetics of fluorescence enhancement at 525 nm (chosen as a representative) upon analyzing different concentrations of Hg^{2+} by the new developed ratiometric fluorescent probe was recorded, and results are shown in Figure 5. The response time of the probe to Hg^{2+} is concentration-dependent, as the time required to reach equilibrium increases with the increase of Hg^{2+} concentrations. However, in all cases, the stable reading could be obtained in less than 2 min. Therefore, this probe could be used for real-time tracking of Hg^{2+} in biological samples. In general, the interaction of porphyrin with metal ion in aqueous solution at room temperature is slow. The fast response of the new probe toward Hg^{2+} might be ascribed to the electronic effect of the naphthalimide moiety on the pyrrole nitrogen atoms of the porphyrin moiety. Moreover, the water solubility of the naphthalimide−porphyrin hybrid improved significantly compared to that of porphyrin alone, which is also beneficial for a fast interaction of the porphyrin moiety with Hg^{2+}. From Figure

Scheme 2. Proposed Binding Mechanism of Probe 1 with Hg^{2+}

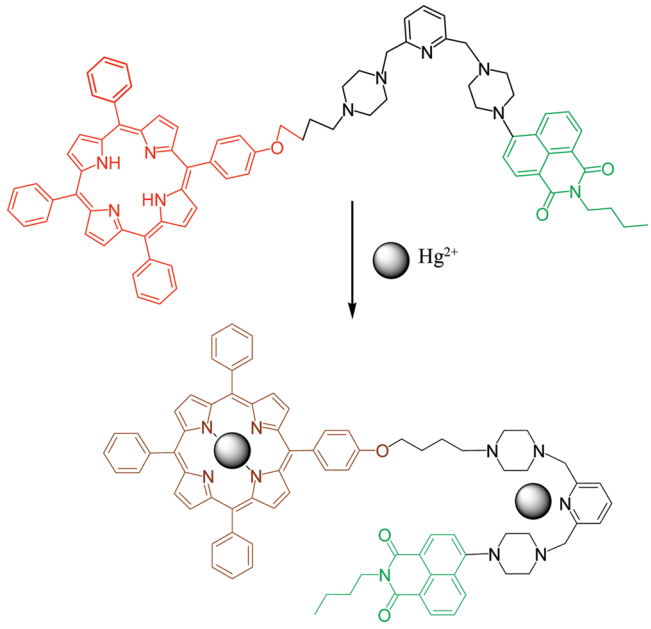

5 one can also discover that once a plateau is reached, the fluorescence intensity at 525 nm stays almost unchanged the rest of the time, indicating that the **1**−Hg^{2+} complex is photostable under irradiation with visible light. The chemical reversibility behavior of the binding of **1** with Hg^{2+} was then studied in the buffed water/ethanol solution. Because of the high stability of the EDTA−Hg^{2+} complex (stability constant log $K_{EDTA\text{-}Hg}$ = 21.5),[21] it could be expected that the addition of EDTA will liberate Hg^{2+} from the metal−ligand complex, releasing free **1**. Therefore, 2 equiv of EDTA (40 μM) was added to the Hg^{2+} (20 μM) complex of **1** (10 μM) in buffered water/ethanol solution, which shows a remarkable decrease of fluorescence signal at 525 nm and an increase of that at 650 nm. The regenerated free **1** can then participate in another Hg^{2+} binding process. These results demonstrate that the Hg^{2+} binding of **1** in buffered water/ethanol solution is chemically reversible, which benefits from the dynamic monitoring of the concentration change of Hg^{2+} in various samples.

Investigation of Sensing Mechanism. To investigate the stoichiometry of the **1**−Hg^{2+} complex, emission spectra data at 525 and 650 nm were first analyzed separately. Experimental emission spectra data indicate the formation of a 1:1 metal−ligand complex for both porphyrin and naphthalimide moiety in **1** with Hg^{2+}, and the association constant is estimated to be 6.31×10^5 M^{-1} for the naphthalimide-linked pyridine moiety and 4.26×10^5 M^{-1} for the porphyrin unit from the emission intensity changes at 525 and 650 nm, respectively (see Supporting Information, Figure S3). Thus, a possible 2:1 metal−ligand structural model for Hg^{2+} and the whole molecule of **1** could be proposed (Scheme 2), in which there exist two sensitive positions. One is the 2,6-bis(aminomethyl)pyridine unit, which adopt a semirigid V-shaped conformation that might be able to selectively bind with a mercury ion.[4b] The other is the porphyrin unit, whose tetrapyrrolic center could coordinate with mercury ion. The interactions of **1** with Hg^{2+} were further studied by ^1H NMR spectroscopy to provide some insights into the interaction mechanism (see Supporting Information, Figure S4). The peaks at around δ = 7.75 ppm, which were assigned to pyridine proton a in free **1**, shift significantly downfield to around δ = 8.03 ppm upon metal coordination. The signals of the protons c, d, and e of the piperazine moiety also undergo a downfield shift upon metal coordination. These deshielding effects confirm the coordination of Hg^{2+} to the N of pyridine and the N of piperazine. In addition, the peak at δ = −2.78 ppm disappeared after the addition of Hg^{2+} ions, which indicates the essential role of Hg^{2+} ions in the tetrapyrrolic center of the porphyrin moiety.

(21) Martell, A. E.; Smith, R. M. *Critical Stability Constants of Metal Complexes*; NIST Standard Reference Database 46; NIST: Gaithersburg, MD, 1993.

Table 1. Recovery Study of Spiked Hg^{2+} in River and Pond Waters with Proposed Probe

sample	Hg^{2+} spiked (μM)	Hg^{2+} recovered, mean[a] ± SD[b] (μM)	recovery (%)
river water 1	1.00	1.04 ± 0.06	104.00
river water 2	5.00	4.81 ± 0.15	96.20
river water 2	20.00	21.33 ± 0.13	105.16
pond water 1	1.00	1.02 ± 0.11	102.00
pond water 2	5.00	5.22 ± 0.21	104.4
pond water 2	20.00	19.44 ± 0.41	97.2

[a] Mean of three determinations. [b] SD: standard deviation.

Preliminary Analytical Application. The practical application of the designed ratiometric fluorescent probe was first evaluated by determination of recovery of spiked Hg^{2+} in river and pond water samples. The river water samples were obtained from the Xiang River (Changsha, China), and pond water samples from the Pond of Taozi at Hunan University (Changsha, China). All the samples collected were simply filtered and showed that no Hg^{2+} was present. In order to reduce the pH influence in the detection, 1 mL of Tris-HCl buffered water was added to 3 mL of the ethanol/water samples (2:1, v/v) containing **1** (10 μM, final concentration) to keep the pH value at 7.0 and then its fluorescence intensity change was detected before and after being spiked with concentrated standard Hg^{2+} solution. The analytical results are shown in Table 1. All the measurements were performed three times. One observed that the results obtained in real water samples show good recovery values, which confirmed that the proposed sensor was applicable for practical Hg^{2+} detection in real samples with other potentially competing species coexisting.

The well-resolved emission spectra of **1** should benefit for observation of fluorescence signal change at two different wavelengths with high resolution, which is especially favorable for ratiometric imaging of Hg^{2+} in biological samples. As a proof-of-concept, a ratiometric confocal fluorescence imaging experiment for Hg^{2+} in living cells was then carried out. Figure 6 showed the double-channel fluorescence images at 515 ± 10 and 650 ± 10 nm. Hela cells incubated with **1** (10 μM) for 1 h showed a strong red intracellular fluorescence (Figure 6a) and a weak green one (Figure 6b), which suggested that **1** was cell permeable. When cells pretreated with compound **1** were further supplemented with $Hg(NO_3)_2$ (10 μM) in PBS for 1 h and washed, a strong quenching of the red fluorescence intensity (Figure 6c) and a remarkable enhancement in the green fluores-

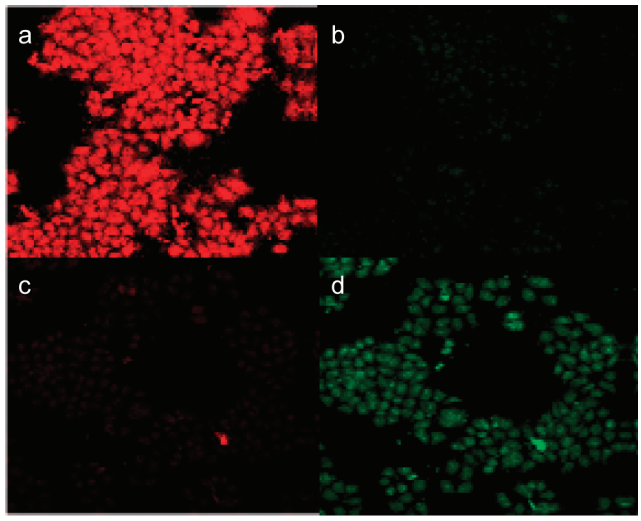

Figure 6. The images of Hela cells incubated by 10 μM compound **1** (a and b) and then further incubated with 10 μM $Hg(NO_3)_2$ (c and d). (the excited light wavelength is fixed at 450 nm, and the emission is centered at 515 $\pm$ 10 nm and 650 $\pm$ 10 nm.

cence intensity (Figure 6d) were observed. The ratio imaging data were obtained using commercial software (Fluoview version 4.3; see Supporting Information, Figures S5 and S6). These preliminary experimental results demonstrate that **1** could be used for ratiometric imaging of Hg^{2+} in biological samples with high resolution.

CONCLUSIONS

In conclusion, we have developed a ratiometric fluorescent probe for Hg^{2+} using a novel strategy by designing a molecule containing two independent Hg^{2+}-sensitive fluorophores with their maximal excitation wavelengths located at the same range. It exhibits a reversibly ratiometric fluorescence response to Hg^{2+} in aqueous solution with high sensitivity and selectivity. The emissions of the two fluorophores in the probe are well-resolved, which benefits for observation fluorescence signal change at two different wavelengths with high resolution and is especially favorable for ratiometric imaging investigations. The recovery test of Hg^{2+} in real water samples and preliminary ratiometric imaging of Hg^{2+} in living cells demonstrate the feasibility of the probe for Hg^{2+} monitoring in practical samples. The results also provide a novel strategy for the design of ratiometric fluorescent probes for other target analytes with well-resolved emission spectra for potential biomedical applications.

ACKNOWLEDGMENT

This work was supported by the National Natural Science Foundation of China (Grant 20505008, 20605007, 20975034), "973" National Key Basic Research Program of China (2007CB310500), Ministry of Education of China (NCET-07-0272), State Key Laboratory of Fine Chemicals (KF0610), and Hunan Natural Science Foundation (07JJ3025).

SUPPORTING INFORMATION AVAILABLE

Additional information as noted in the text. This material is available free of charge via the Internet at http://pubs.acs.org.

Received for review August 15, 2009. Accepted November 3, 2009.

AC9018445